Microchimica Acta (2020) 187: 225
https://doi.org/10.1007/s00604-020-4203-1

ORIGINAL PAPER

Functionalized magnetic nanomaterials for electrochemical biosensing of cholesterol and cholesteryl palmitate

Rodica Doaga[1] · Timothy McCormac[2] · Eithne Dempsey[3]

Received: 11 October 2019 / Accepted: 28 February 2020 / Published online: 13 March 2020

Abstract

Synthesis and functionalization of magnetite nanoparticles (Fe_3O_4) was achieved with the view to covalently bind both cholesterol oxidase and cholesterol esterase biorecognition agents for the development of free and total cholesterol biosensors. Prior to enzyme attachment, Fe_3O_4 was functionalized with 3-aminopropyltriethoxysilane (APTES) and polyamidoamine (PAMAM) dendrimer. Characterization of the material was performed by FT-IR and UV spectroscopy, SEM/EDX surface analysis and electrochemical investigations. The response to cholesterol and its palmitate ester was examined using cyclic voltammetry. Optimum analytical performance for the free cholesterol biosensor was obtained using APTES-functionalized magnetite with a sensitivity of 101.9 μA mM^{-1} cm^{-2}, linear range 0.1–1 mM and LOD of 80 μM when operated at 37 °C. In the case of the total cholesterol biosensor, the best analytical performance was obtained using PAMAM dendrimer-modified magnetite with sensitivity of 73.88 μA mM^{-1} cm^{-2} and linear range 0.1–1.5 mM, with LOD of 90 μM. A stability study indicated that the free cholesterol biosensors retained average activity of 98% after 25 days while the total cholesterol biosensors retained 85% activity upon storage over the same period.

Keywords Magnetite (Fe_3O_4) · APTES (3-aminopropyltriethoxysilane) · PAMAM (polyamidoamine dendrimer) · Cholesterol oxidase · Cholesterol esterase · Cholesterol biosensor

Introduction

The clinical analysis of cholesterol in serum samples is important in the diagnosis and prevention of a large number of clinical disorders. In conditions such as atherosclerosis, hypothyroidism, nephrosis, diabetes mellitus, myxedema and obstructive jaundice, the patient will have increased levels of cholesterol and its esters above the physiological norm. Decreased levels are found in patients suffering from hyperthyroidism, anaemia, malabsorbtion and wasting syndromes. The desired total plasma cholesterol for an individual is less than 5.2 mM (200 mg dl^{-1}), with a high level being considered as greater than 6.2 mM (240 mg dl^{-1}). Plasma cholesterol levels increase with age and are generally less in women than men [1].

In relation to biosensing, immobilization of cholesterol oxidase (ChOx) and/or cholesterol esterase (ChEs) enzymes onto suitable transducers is a selective means of cholesterol determination though signals obtained that are usually very small (a few nanoamperes), due to the low enzymatic activity (typically 2.5 U mg^{-1} solid and 3.5 U mg^{-1} solid for ChOx and ChEs, respectively) [2]. The sequence of the typical bienzyme reaction is shown below, followed by electrooxidation of the so-produced hydrogen peroxide:

$$\text{Cholesterol Esters} + H_2O \xrightarrow{\text{ChEs}} \text{Cholesterol} + \text{Fatty Acids} \quad (1)$$

$$\text{Cholesterol} + O_2 \xrightarrow{\text{ChOx}} \text{Cholest-4-en-3-one} + H_2O_2 \quad (2)$$

Motonaka et al. described the application of [Os $(bpy)_3](PF_6)_2$/acetylene black-teflon emulsion deposited on Pt electrode for the development of free and total cholesterol biosensors [3]. The resulting biosensors offered a narrow linear range for free cholesterol up to 0.47 mM, and to 1 mM for the total cholesterol biosensor. Limited linear range resulted for the free cholesterol biosensor described by Zhou et al., up

✉ Eithne Dempsey
eithne.dempsey@mu.ie

[1] Centre of Applied Science for Health (CASH), Technological University Dublin, Tallaght Campus, Dublin 24, Ireland

[2] Dundalk Institute of Technology, Dundalk, Co., Louth, Ireland

[3] Department of Chemistry, Kathleen Lonsdale Institute for Human Heath Research, Maynooth University, Maynooth, Ireland

to 50 μM respectively, based on Au nanoparticles-cysteamine [4]. The use of cyclic voltammetry for the analysis of cholesterol was reported by Kumar et al. and Aravamudhan et al., based on PPy-dodecylbenzene sulfonate polymer film on ITO (indium tin oxide) and thioctic acid (SAM) on Au electrode respectively [5, 6], with sensitivity of 69 nA mM^{-1}.

Nanomaterials provide high surface areas and a biocompatible environment for enzyme loading with toxicity, chemical stability and high electron transfer capability being of significance. In the last decade, the investigation of magnetic particles has resulted in their usage in numerous nanosensing devices, allowing ease of separation in solution. Functionalized magnetic nanoparticles can also be directed by an external magnetic field to site-specific drug delivery targets. Hasanzadeh et al. have reviewed iron and iron oxide nanoparticles as signal amplification elements in biosensing [7]. Among these materials, magnetite (Fe_3O_4), a Fe^{2+} and Fe^{3+} complex oxide, is one of the most commonly studied super-paramagnetic nanoparticle. It has unique mesoscopic physical and mechanical properties and has many potential applications in several fields such as microwave absorption [8] and cell separation [9]. Fe_3O_4 nanoparticles have been widely used for in vivo examination including magnetic resonance imaging, contrast enhancement, tissue specific release of therapeutic agents, magnetic field assisted radionuclide therapy and surface assisted laser desorption mass spectrometry [10], as well as in vitro binding of proteins and enzymes [11].

Due to its good biocompatibility, strong superparamagnetism, low toxicity and easy preparation process, Fe_3O_4 has recently been employed in biosensors for glucose, ethanol and acetaminophen [12, 13] and in immobilization of many bioactive substances such as proteins, peptides, enzymes and antibodies [11, 14]. The binding of magnetic particles to bioactive substances involves a number of interactions including interactions between the organic ligand and between the amino acid side chains of proteins and the metal centres [11]. Magnetic nanoparticles have been functionalized with amino-silane and polyamidoamine (PAMAM), the latter introducing a dense outer amine shell through a cascade-type generation. Such bindings pave the way for the coupling of biomolecular entities of enhanced stability. Ahmad et al. reported cholesterol oxidase Pt incorporated ZnO hybrid nanospheres, which were formed via electrodeposition and enzyme adsorption [15]. The material exhibited a rapid sensitive response (1886 mA M^{-1} cm^{-2}) up to 15 μM cholesterol. Recently, Huang et al. developed a cholesterol biosensor based on enzyme modified gold nanoparticles with quantitation enabled via reduction of silver ions by enzymatically generated H_2O_2 [16]. Other examples of cholesterol biosensing which exploit nanoparticles include nanoscale Pt nanoparticles and graphene [17]. Prussian blue encapsulated iron oxide nanostructures [18], a paper based cholesterol biosensor based on graphene/polyvinylpyrroliidone/polyaniline nanocomposites [19] and core shell silica nanocomposite, was used to immobilize cholesterol oxidase, esterase and horseradish peroxidase [20].

In this article, the synthesis and functionalisation of magnetite nanoparticles with 3-aminopropyltriethoxysilane (APTES) and PAMAM were achieved with subsequent covalent attachment of both cholesterol oxidase and cholesterol esterase. Enzyme binding confirmation involves the use of a protein assay, surface analysis and electrochemical studies. The functionalized nanomaterials prepared here provide a new approach to electroanalysis of both cholesterol and cholesterol esters, which to the best of our knowledge has not yet been reported. The amino-silane initiator core provides for dendrimer growth with multiple enzyme attachment sites per Fe_3O_4 particle. Features such as excellent stability and flexible preparation methodologies are advantageous properties (e.g. control of dendrimer formation), enabling an extension of the range of clinical targets for biosensing applications.

Experimental

Materials

Iron salts—$FeCl_2$, $FeCl_3$, ammonium hydroxide 30%, Triton X 100, Nafion solution 5%, KCl, KH_2PO_4, K_2HPO_4, 3-aminopropyltriethoxysilane (APTES), poly(amidoamine) dendrimer (G4-PAMAM), methylacrylate, ethylenediamine, methanol, ethanol, 25% aqueous glutaraldehyde, cholesterol, cholesteryl palmitate, cholesterol oxidase (ChOx, 2.4 U mg-1 solid) and cholesterol esterase (ChEs, 3.6 U mg^{-1} solid), were from Sigma-Aldrich (www.sigmaaldrich.com).

Apparatus

Cyclic voltammetry and amperometry experiments were carried out using CH Instruments CHI 900. Platinum electrodes (area = 0.0314 cm^2), Ag/AgCl reference electrode for aqueous solutions, a platinum counter electrode and a three compartment cell were from CHI Instruments. Substrate solutions were prepared using a thermostated bath, sonication was performed using a Branson 2510 sonicator, drying of the functionalized magnetite was carried out in a thermostated oven WTB Binder from Germany, UV studies were carried out using UV-160A (Shimadzu), IR analysis was carried out using a Nicolet Avatar 320 FT-IR spectrometer and SEM images were obtained using a Hitachi S-2400N system.

Synthesis of magnetic nanoparticles

Magnetic nanoparticles (MNP) were prepared by the chemical co-precipitation method followed by treatment under hydrothermal conditions. Briefly, iron(II) chloride and iron(III) chloride (1:2) were chemically precipitated at room

temperature (25 °C) by adding ammonium hydroxide 30% at a controlled pH = 10.0–10.4. The precipitates were heated at 80 °C for 35 min under continuous mixing and washed in deionized water and in ethanol [11]. Surface hydroxyl groups of the resultant nanoparticles enabled different approaches for the coupling of biomolecular entities [21].

Synthesis of APTES-functionalized magnetite

A total of 1.3 g freshly synthesized magnetite was dissolved in 30 mL ethanol and sonicated for 30 min. Ten millilitre of the dispersed magnetite was added to 0.5 mL APTES and sonicated for a further 10 min. The mixture was then stirred overnight at room temperature. The APTES-functionalized magnetic nanoparticles were recovered from the reaction mixture by placing the bottle on a permanent magnet with a strong surface magnetisation. The precipitate was washed several times with ethanol and then with deionized water and dried in an oven [22]. A 50 mg sample of APTES-coated magnetite nanoparticles was dispersed in 10 mL aqueous solution of 5% glutaraldehyde (GA) and then stirred at room temperature (25 °C) for 3 h. After settling, the APTES-glutaraldehyde-modified magnetite nanoparticles were washed with deionized water several times in order to remove unreacted GA. The APTES-functionalized MNP were stored at 4 °C.

Synthesis of PAMAM-dendrimer functionalized magnetite

A total of 20 mL of the ethanol-dispersed magnetite was added to 4 mL APTES (3-aminopropyltriethoxysilane) and sonicated for a further 10 min. The mixture was then stirred for 3 h at room temperature. A 200 mL sample of 20% (v/v) solution of methylacrylate in methanol was added to the dispersed APTES magnetite solution. This was stirred for 7 h in order to enhance the binding, and the particles were collected magnetically and washed with methanol five times by magnetic separation. After rinsing, 40 mL of 50% (v/v) ethylenediamine methanol solution was added and the suspension was sonicated at room temperature for 3 h. The resulting particles were rinsed with methanol five times by magnetic separation. Stepwise growth using methylacrylate and ethylenediamine was repeated five times until the PAMAM dendrimer (five generation) was generated [23] (see Scheme 1).

The final solution was washed with methanol (× 5) and then with deionized water. The PAMAM-functionalized magnetite nanoparticles were dispersed in 10 mL aqueous solution of 5% glutaraldehyde (GA) and stirred at room temperature (25 °C) for 3 h. After settling, the magnetite nanoparticles were washed with deionized water several times in order to remove the unreacted GA. The PAMAM dendrimer-functionalized MNP (magnetic nanoparticles) were stored at 4 °C.

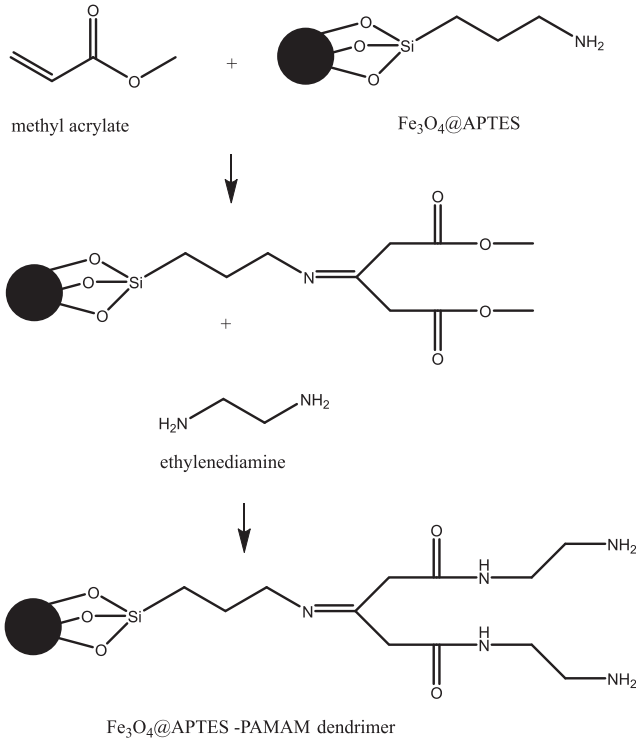

Scheme 1 PAMAM dendrimer formation at APTES-functionalized Fe_3O_4 core. Coupling of terminal amine groups with glutaraldehyde subsequently enabled enzyme attachment

Enzyme binding

In the case of free cholesterol biosensor, 2.5 mg of cholesterol oxidase (ChOx) was mixed with 30 μL of phosphate buffered saline with 0.1 M KCl (PBS) and 10 μL of APTES or PAMAM dendrimer-functionalized magnetic nanoparticles. For the total cholesterol biosensor, 1 mg ChOx and 1 mg ChEs (cholesterol esterase) were added to 20 μL of the APTES or PAMAM dendrimer-modified magnetic nanoparticles. The final mixtures were sonicated for approximately 30 min at 4 °C and then 5 μL was drop cast onto the Pt transducer surface [24, 25].

The free and total cholesterol biosensors were analysed with an additional thin layer of 5 μL Nafion solution (1% in methanol), in order to provide further stability. As additional controls, free and total cholesterol biosensors were also formed in the absence of MNP, using the same amounts of enzyme crosslinked with glutaraldehyde [22, 23]. All biosensors were stored at 4 °C for 24 h before use.

Bradford assay

The colorimetric method was performed firstly on BSA (bovine serum albumin) in order to obtain a calibration plot at 595 nm. Then 1 mg of ChOx was mixed with different quantities of APTES/PAMAM-functionalized MNP (0.5, 1.0 and 1.5 mg mL^{-1}). Following binding, the mixtures were washed

with deionized water and 1 mL of Bradford reagent was added. The colorimetric assay was based on the observation that the absorbance maximum for an acidic solution of Coomassie Brilliant Blue G-250 shifted from 465 nm to 595 nm when binding to protein occured. Both hydrophobic and ionic interactions stabilize the anionic form of the dye, causing a visible colour change [11].

Preparation of stock solutions

Stock solutions of 10 mM cholesterol or cholesteryl palmitate were employed. The stock solutions were made up in 50 mM PBS (pH = 7.00) containing 10% (v/v) Triton X-100, in a thermostated bath at 65 °C under continuous stirring for approximately 1 h. Both solutions were stored at 4 °C in the dark, until a slight turbidity was observed.

Results and discussion

Spectroscopic characterization

In the case of pure magnetite, FTIR spectroscopy was used in order to obtain information about the nature of surface hydroxyl groups and adsorbed water. Adsorbed water molecules can result in a surface covered by hydroxyl groups coordinated to the underlying Fe atoms. Hydroxylation of iron oxides is a fast reaction requiring minutes, and it is followed by further adsorption of water molecules which interact via H bonding to the surface OH groups. The surface hydroxyl groups, arising from either adsorption of water or from structural OH, are the functional groups of iron oxides [21].

An experiment was performed in order to confirm the identity of the peak at 1622 cm^{-1} as a surface OH group as per literature [21]. It was confirmed that by drying the magnetite at different temperatures (50 to 800 °C), the band at 1622 cm^{-1} gradually decreased in intensity and it disappeared completely at temperatures higher than 800 °C (spectra not shown here).

Figure 1a shows the FTIR for APTES-modified magnetite and enzyme-bound magnetite spectra. The Si–O stretch appeared at typical frequencies of approximately 1080 cm^{-1} and is probably influenced by neighbouring Fe atoms. Upon glutaraldehyde binding, the spectrum of MNP-APTES showed an absorption band at 1640 cm^{-1}, which was attributed to C=O from glutaraldehyde or unbound primary amine N–H. Following enzyme binding, the absorption band shifted from 1640 to 1643 cm^{-1} indicating attachment of the protein. The spectrum of pure enzyme (ChOx) in deionized water showed an absorption band at 1640 cm^{-1} attributed to amide I and 1554 cm^{-1} characteristic of amide II from proteins (spectrum not shown here). Unfortunately, the amide II characteristic band from proteins was not observed in the enzyme bound MNP spectrum probably due to the low quantity of protein

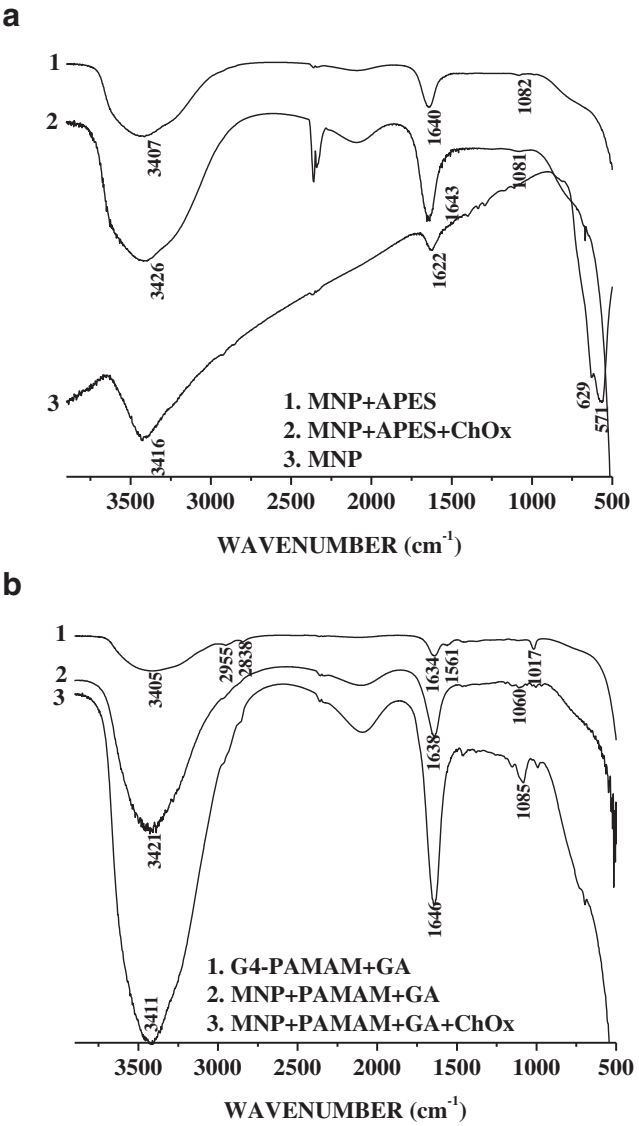

Fig. 1 **a** FT-IR spectra of pure MNP (3), 3-aminopropyltriethoxysilane (APTES)-functionalized MNP (1) and APTES/Cholesterol oxidase bound MNP (2). **b** FT-IR spectra of pure G4-PAMAM (1) and PAMAM-functionalized MNP (2) after GA activation and the cholesterol oxidase-PAMAM-bound MNP (3)

present. The band at 2400 cm^{-1} was attributed to tertiary amine, more visible in the MNP-APTES-ChOx spectrum. The typical Fe–O signal from magnetite itself was observed at 629 cm^{-1} and 571 cm^{-1} (Fig. 1a).

Figure 1b shows the overlaid spectra of pure dendrimer G4-PAMAM (commercially available), PAMAM-functionalized MNP and cholesterol oxidase-PAMAM-bound MNP. Both MNP-PAMAM and G4-PAMAM show the carbonyl and amine absorption bands as one amide I band—its position depends on the degree of hydrogen bonding. Thus, the absorption band shifted from 1629 to 1638 cm^{-1} in the case of MNP-PAMAM-GA, and from 1646 to 1634 cm^{-1}. In the case of G4-PAMAM-GA, the

amide II band was in the same position at 1561 cm^{-1}. Binding can also be confirmed by the shift in the band from 3405 to 3332 cm^{-1}. Small shifts occurred also for Si–O stretching vibrations, and the Fe–O bands disappeared completely or shifted to lower frequencies possibly due to the influence of neighbouring atoms such as Si. After enzyme attachment, the characteristic absorption band for amide I shifted from 1638 to 1646 cm^{-1}, confirming the immobilization of cholesterol oxidase on Fe_3O_4. The amide II band was not obvious, possibly due to a hindrance caused by the broad amide I [23].

Enzyme binding efficiency was determined by assaying the protein bound to magnetite using the Bradford assay (see 'Bradford assay'). It can be concluded that the enzyme (ChOx) bound more efficiently with APTES-functionalized magnetite, with 96.6% binding efficiency, compared with the PAMAM-modified magnetite, with 83% efficiency. The electroanalytical performances of the biosensors as well as the SEM analysis represent further evidence of successful enzyme binding.

SEM analysis

SEM analysis was performed on the magnetite nanoparticles in order to determine their size and morphology. The size of the magnetic nanoparticles varied from 10 to 100 nm, and they are more likely to aggregate because of their large surface area to volume ratio and strong magnetic dipole-dipole attractions between particles [10]. Figure 2 a and b show the SEM images obtained for APTES-modified magnetite and the bound-enzyme magnetite. In the case of the bound-enzyme image from Fig. 2b, it was noticed that the immobilization of enzyme to the APTES-functionalized nanoparticles resulted in aggregation into circular microstructures with average diameters of approximately 1 μm. The aggregation process could be explained by the fact that the binding may involve several molecules of cholesterol oxidase on a single Fe_3O_4 particle or that cholesterol oxidase molecules were bonded to several magnetic nanoparticles [21].

Figure 2c shows the SEM analysis of enzyme loaded PAMAM-modified magnetite indicating excellent binding efficiency to the PAMAM-functionalized nanoparticles which resulted in a regular dispersion of enzyme loaded microstructures. The binding resulted in nicely dispersed particles of typically 500 nm (1 μm average diameter in the case of APTES-MNP). It can be concluded that the presence of the dense outer amine shell of the dendrimer contributed to more efficient enzyme binding and possibly binding involved several magnetic nanoparticles [21]. Figure 2d shows the EDX spectrum for Fe_3O_4 indicating the dominance of Fe and O signals.

Electroanalytical characterization of cholesterol biosensors

Cyclic voltammetry in PBS, pH = 7.00 solution, was used for biocatalytic studies, performed in a 3 mL electrochemical cell at both room temperature (Fig. 3a–d) and 37 °C (results not shown here). The response from 0.6 V vs. Ag/AgCl was due to direct oxidation of hydrogen peroxide produced as a result of the enzyme-substrate reaction. The cyclic voltammograms were obtained at the modified platinum electrodes vs. Ag/AgCl at scan rate 5 mV/s, in the absence (solid line) and presence (dotted line) of substrate.

Figure 3 a and b show cyclic voltammograms generated in the presence of 1.5 mM cholesterol at room temperature, using the APTES and PAMAM-functionalized magnetite on Pt electrodes. The free cholesterol biosensors realized electrooxidation of hydrogen peroxide at a potential of approximately 0.65 V vs. Ag/AgCl, as a result of the conversion of cholesterol to cholest-4-en-3-one and hydrogen peroxide.

Figure 3 c and d show cyclic voltammetric response to increasing concentration of cholesteryl palmitate at room temperature—APTES and PAMAM-functionalized magnetite on Pt electrode. The total cholesterol biosensors resulted in hydrogen peroxide oxidation at a potential of approximately 0.70 V vs. Ag/AgCl. The hydrolysis of cholesterol esters (in this case cholesterol palmitate) is catalysed by the enzyme cholesterol esterase in order to produce free cholesterol and fatty acids. Subsequently, the free cholesterol was oxidized by cholesterol oxidase to produce cholest-4-en-3-one and hydrogen peroxide (Eqs. (1) and (2)). The results indicate that the peak currents were proportional to the concentration of cholesteryl palmitate present in the electrochemical cell.

Figure 4 a and b show increased currents generated by the free cholesterol biosensor as a function of the concentration of cholesterol at 37 °C using the APTES and PAMAM-functionalized magnetite on Pt electrode. Figure 4 c and d show cyclic voltammograms for the total cholesterol biosensor response to cholesteryl palmitate at 37 °C using both types of functionalized magnetic nanoparticles on Pt electrode. The corresponding calibration plots for free cholesterol using the MNP-APTES, MNP-PAMAM and the control electrode (at room temperature and 37 °C) are shown in Fig. 5 a and b. We can conclude that the widest linear range was obtained for the biosensor prepared using cholesterol oxidase bound to APTES-functionalized magnetite at room temperature and at 37 °C. The activity of enzyme was calculated taking into account the efficiency of binding. The control sensor represents the direct binding of cholesterol oxidase (0.75 U) through glutaraldehyde in the absence of magnetite. The increased linear range of the MNP bound enzyme relative to the control electrode indicated a more heterogeneous surface with more controlled diffusion of substrate to the biocatalytic layer. In both cases, sensitivity was enhanced for the APTES-MNP relative to the PAMAM reflecting the lower enzyme activity.

Figure 5 c and d show the performance of the total cholesterol using the MNP-APTES, MNP-PAMAM and the control electrode at room temperature and 37 °C, respectively. Due to the different binding affinities of the materials, there is a difference

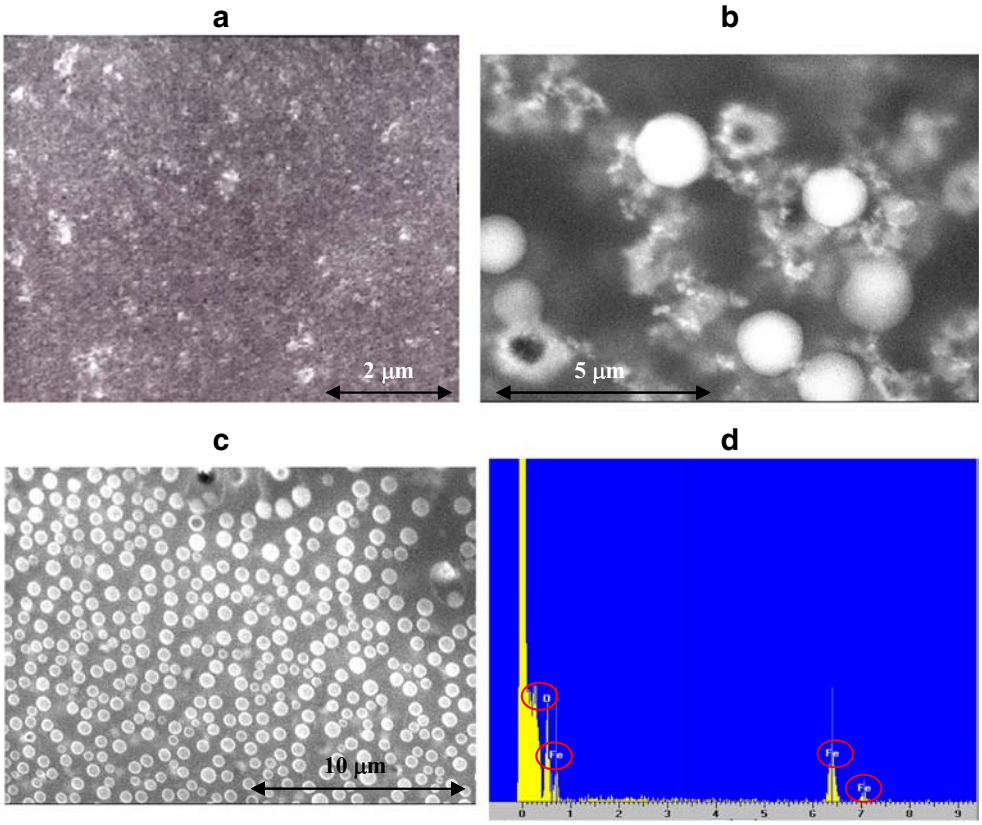

Fig. 2 **a** SEM image of APTES-MNP, magnification × 20 K, accelerating voltage of 10 kV, resolution 2 μm. **b** SEM image of APTES-MNP bound to cholesterol oxidase, magnification X10 K, accelerating voltage of 18 kV, resolution 5 μm. **c** SEM image of PAMAM-MNP, magnification × 30 K, accelerating voltage of 18 kV, resolution 1 μm. **d** EDX of Fe_3O_4 indicating the dominance of Fe and O signals

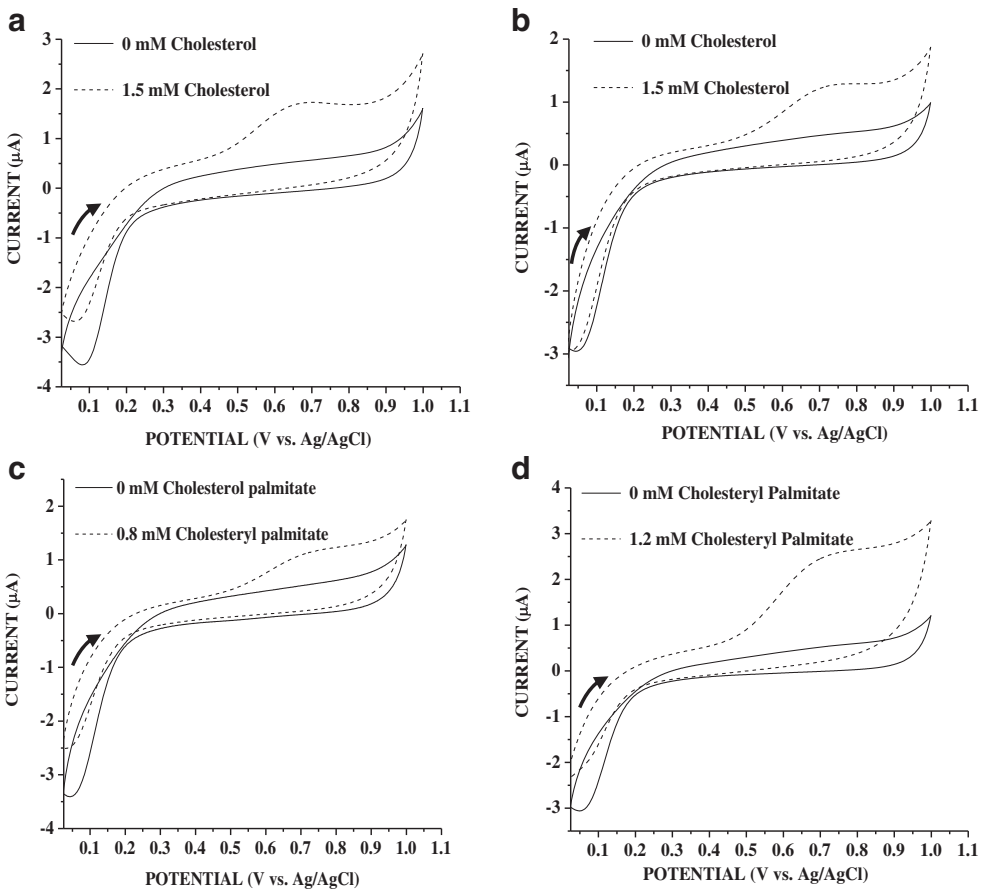

Fig. 3 **a** Cyclic voltammograms obtained for free cholesterol biosensor at R.T. using the APTES-functionalized nanoparticles in PBS at scan rate 5 mV/s vs. Ag/AgCl in the absence (solid line) and presence of 1.5 mM cholesterol (dotted line). **b** CVs for free cholesterol biosensor at R.T. using the PAMAM dendrimer-functionalized nanoparticles under the same conditions as **a** in the absence (solid line) and presence of 1.5 mM cholesterol (dotted line). **c** CVs obtained for total cholesterol biosensor at R.T. using the APTES-functionalized nanoparticles (conditions as **a**) in the absence (solid line) and presence of 0.8 mM Cholesteryl palmitate (dotted line). **d** CVs for total cholesterol biosensor at R.T. using the PAMAM-functionalized nanoparticles in the absence (solid line) and presence of 1.2 mM Cholesteryl palmitate (dotted line)

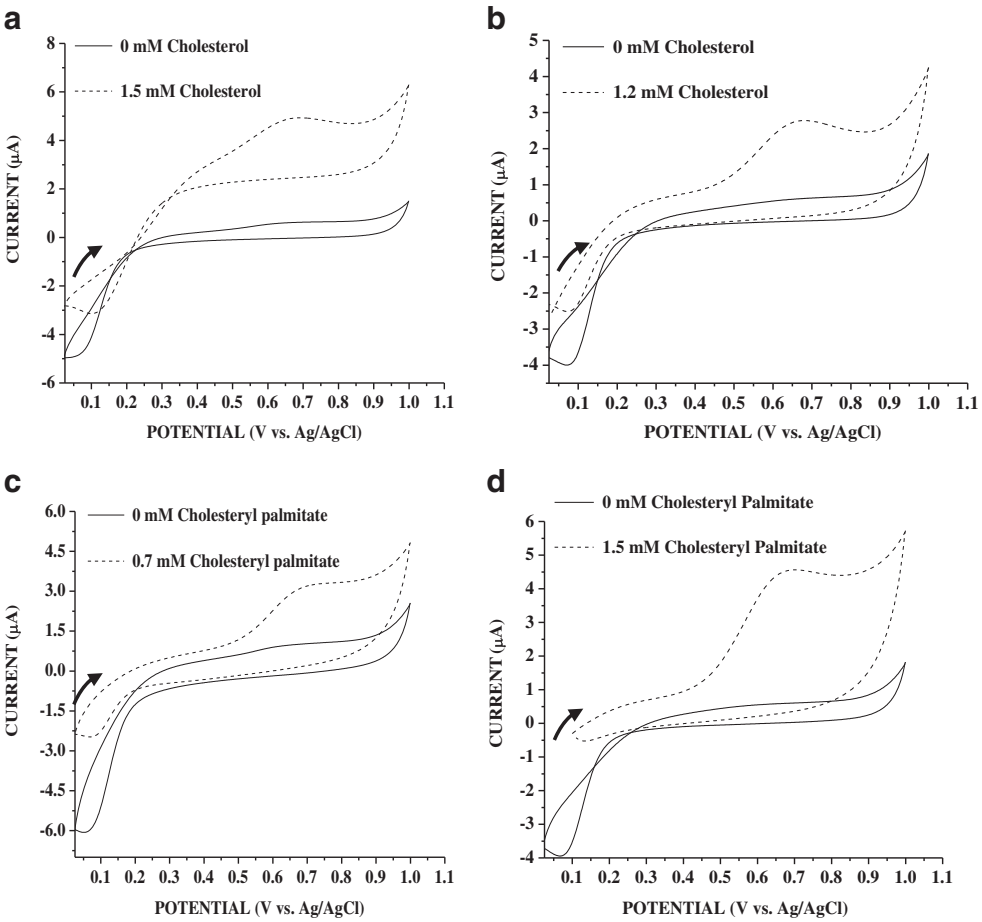

Fig. 4 **a** Cyclic voltammograms obtained for free cholesterol biosensor at 37 °C using the APTES-functionalized nanoparticles in PBS vs. Ag/AgCl at scan rate 5 mV/s, in the absence (solid line) and presence of 1.5 mM cholesterol (dotted line). **b** CVs for the free cholesterol biosensor at 37 °C using PAMAM dendrimer-functionalized nanoparticles under same conditions as **a**, in the absence (solid line) and presence of 1.2 mM Cholesterol (dotted line). **c** CVs obtained for total cholesterol biosensor at 37 °C using the APTES-functionalized nanoparticles under same conditions as **a**, in the absence (solid line) and presence of 0.7 mM cholesteryl palmitate (dotted line). **d** Cyclic voltammograms obtained for total cholesterol biosensor at 37 °C using the PAMAM-functionalized nanoparticles under same conditions as **a**, in the absence (solid line) and presence of 1.5 mM cholesteryl palmitate (dotted line)

in surface enzyme activity of cholesterol oxidase and esterase. From the above data, we can conclude that the best linear range was obtained for the biosensors prepared using cholesterol oxidase and cholesterol esterase bound to PAMAM-functionalized magnetite at both, room temperature and 37 °C. Normal values for free cholesterol in blood are between 1.00 and 2.00 mM, while abnormal values are > 2.00 mM. As the desired total plasma cholesterol for a patient is less than 5.2 mM, and a high level is considered as greater than 6.2 mM. Therefore, in the case of these sensing surfaces, real samples will require dilution prior to analysis. Mediator attachment to the Fe_3O_4 particles coupled with outer/inner layer polymeric selectivity configurations could possibly improve the linear range, and at the same time eliminate direct electrochemical interference from other species present in blood samples.

In relation to reproducibility, the free cholesterol response to 1.5 mM cholesterol resulted in 0.4% coefficient of variation ($n = 3$) while total cholesterol (response to 0.5 mM cholesterol palmitate) gave a coefficient of variation of 15.3% ($n = 3$) the difference possibly due to the bienzyme cascade and lower concentration used.

Table 1 summarizes analytical parameters obtained at both room temperature and 37 °C. The enhanced analytical performance of the PAMAM-functionalized magnetite is possibly due to the high surface area material on the electrode surface with multiple binding sites available for protein attachment. The lowest linear range (0.1–0.5 mM) was obtained for the control biosensors prepared in the absence of magnetite (enzyme attachment via GA only). With respect to sensitivity, the best performance was obtained for the free cholesterol biosensor using the APTES-MNP, with a sensitivity value of 102 μA mM^{-1} cm^{-2}, R^2 of 0.9960 when operated at 37 °C, followed by comparable results obtained for total cholesterol biosensors, using APTES (78.66 μA mM^{-1} cm^{-2} $R^2 = 0.9832$) and PAMAM-functionalized magnetite (73.88 μA mM^{-1} cm^{-2} $R^2 = 0.9974$) both operated at 37 °C. A lower sensitivity of 68.15 μA mM^{-1} cm^{-2} was obtained for the direct binding with GA, in the absence of MNP, although the activity of enzyme was higher compared with the functionalized materials.

The overall performance of both materials compared very favourably in relation to sensitivity relative to total cholesterol reports based on similar nanomaterials (see Table 2) for analytical comparison with relevant literature. Two articles have been published which reported similar results in terms of linear ranges to those described here, but with lower sensitivities. Ruiz et al. applied poly-diaminonaphthalene on a Pt disk and cholesterol oxidase as well as cholesterol esterase in order to develop an amperometric biosensor [24]. The working

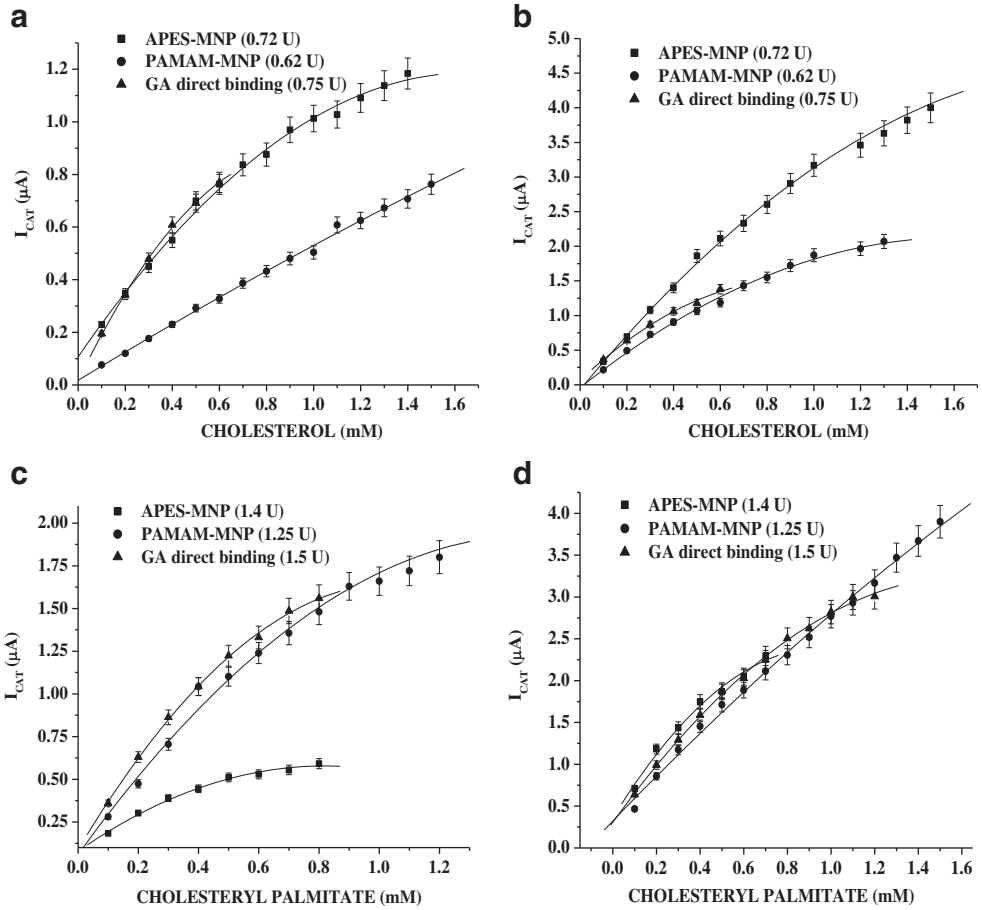

Fig. 5 **a** Calibration curves for free cholesterol biosensors obtained using ChOx bound to APTES-functionalized magnetite, PAMAM-functionalized magnetite and control ChOx sensor at R.T. in PBS, standard additions of 0.1 mM cholesterol. error bars are standard deviation for $n = 3$. **b** Calibration curves for free cholesterol biosensors obtained using ChOx bound to APTES-functionalized magnetite, PAMAM-functionalized magnetite and control ChOx sensor at 37 °C in PBS, standard additions of 0.1 mM cholesterol. Error bars are standard deviation for $n = 3$. **c** Calibration curves for total cholesterol biosensors obtained using ChOx and ChEs bound to APTES-functionalized magnetite, PAMAM-functionalized magnetite and control sensor at R.T. in PBS, standard additions of 0.1 mM cholesterol. Error bars are standard deviation for $n = 3$. **d** Calibration curves for total cholesterol biosensors obtained using ChOx and ChEs bound to APTES-functionalized magnetite, PAMAM-functionalized magnetite and control sensor at 37 °C in PBS, standard additions of 0.1 mM cholesterol. Error bars are standard deviation for $n = 3$

Table 1 Analytical parameters for free and total cholesterol biosensors using APTES- and PAMAM-functionalized MNP, at both room temperature and 37 °C

Analytical parameter	Fe_3O_4@APTES (0.72 U)		Fe_3O_4@PAMAM (0.62 U)	
	Room temperature	37 °C	Room temperature	37 °C
Linear range (mM)	*0.1–1.0	0.1-1.0	0.1–1.5	0.1–1.0
	&0.1-0.5	0.1-0.7	0.1–0.8	0.1–1.5
Sensitivity ($\mu A\ mM^{-1}\ cm^{-2}$) n = 3	*28 ± 1.27	*101.9 ± 2.8	*15.6 ± 0.32	*56.36 ± 1.68
	&25.47 ± 0.73	&78.66 ± 3.44	&52.55 ± 2.86	&73.88 ± 2.48
LoD (μM)	*100	80	80	90
	&80	100	100	100
R^2	*0.9889	0.9960	0.9983	0.9965
	&0.9882	0.9832	0.9834	0.9974

* Free cholesterol

& Total cholesterol

Table 2 Comparative performance study for reported cholesterol biosensors (total cholesterol oxidase and esterase bienzyme systems)

Electrode	Sensitivity (μA mM^{-1} cm^{-2})	Linear range (mM)	Reference
Fe_3O_4@C@AgNPs (total cholesterol bienzyme)	0.0346	0.5–22.5	[20]
Graphene-Pt nanoparticle hybrid (total cholesterol bienzyme)	2.07	0.05–0.030	[17]
PANI	4.9×10^{-5} (μA mM^{-1})	0.76–7.67	[26]
Ti/NPAu	29.33	1.04–7.8	[27]
SPE/Fe_3O_4	100.2 (μA mM^{-1})	1.5–6.14	[28]
Fe_3O_4@APTES-MNP	25.49	0.1–0.7	This work
Fe_3O_4@PAMAM-MNP	52.55	0.1–0.8	This work

potential was 0.7 V vs. Ag/AgCl, up to 0.8 mM with a sensitivity of 0.39 nA mM^{-1}. The total cholesterol sensor developed by Salinas et al. consisted of a rotating disk with both enzymes entrapped into 3-aminopropyl-modified controlled-pore glass, operated at − 0.15 V vs. Ag/AgCl, over the range 1.2–1000 μM, with sensitivity of approximately 70 nA mM^{-1} [25]. Overall, the novel approach exploited and demonstrated herein provides for a sensitive robust response to both cholesterol and its ester, having its foundation in functionalized magnetic nanoparticles, enabling enzyme loading with improved dispersion of resultant nanocomposite materials.

Stability studies

The use of a biosensor is normally limited to the lifetime of the immobilized enzyme and therefore electrodes were tested for a period of 50 days. The free cholesterol biosensor was prepared using APTES-functionalized magnetite and the total cholesterol biosensor using PAMAM dendrimer-functionalized magnetite. Two electrodes were employed: one stored at room temperature and one at 4 °C. Cyclic voltammograms were carried out at 37 °C in PBS with addition of 0.5 mM cholesterol and 0.8 mM cholesteryl palmitate. The free cholesterol biosensor stored at room temperature and 4 °C resulted in the highest stability, retaining an impressive average of 98% activity after 25 days. The total cholesterol biosensors stored at room temperature and 4 °C showed slightly lower stability of 85%, probably due to the dual enzyme component of the total cholesterol device. In comparison to literature, variations in long-term stability are reported with Malik et al. [29], Kumar et al. [5] and Marazuela et al. [30], demonstrating that the cholesterol biosensors developed were stable for 1–3 months. The biosensors were based on acrylamine glass beads, tetraethylorthosilicate-derived sol gel and ruthenium (II) complex (3 months), respectively.

Conclusions

Magnetic nanoparticles were synthesized by the thermal co-precipitation method using ferric and ferrous chlorides and functionalized using APTES and PAMAM with subsequent covalent attachment of cholesterol esterase and cholesterol oxidase. The binding efficiency of the enzyme was analysed by FT-IR and UV spectroscopy and confirmed by SEM surface analysis and electrochemical investigations. Determination of free cholesterol and total cholesterol using the magnetite-modified biosensors offers the possibility of clinical analysis of cholesterol in serum samples based on this novel method of enzyme immobilization on magnetite. The sensors resulted in improved or comparable analytical performance with respect to current methods possibly due to enhanced access and diffusion of substrates to the enzyme's active site, together with conformational stability and activity of immobilized enzymes. The 3-aminopropyltriethoxysilane and especially the polyamidoamine dendrimer's ability to form a dense outer amine shell resulted in an efficient enzyme binding as confirmed by SEM, Bradford assay and biocatalytic response.

The optimum analytical performance for the free cholesterol biosensor was obtained using APTES-functionalized magnetite with a sensitivity of 101.9 μA mM^{-1} cm^{-2}, linear range of 0.1–1 mM and R^2 of 0.9960 when operated at 37 °C. For the total cholesterol biosensor, the best analytical performance was obtained using PAMAM dendrimer-modified magnetite with a sensitivity of 73.88 μA mM^{-1} cm^{-2} linear range 0.1–1.5 mM, with R^2 of 0.9974. The stability study showed that the free cholesterol biosensors were more stable than the total cholesterol biosensors with retained activity of 98% after 25 days. In conclusion, this research demonstrates the ability to covalently attach enzymes to functionalized materials with specific response to cholesterol and its ester which demonstrates improved stability, linearity and comparable sensitivity to existing methods. Further work will examine the entrapment/attachment of mediators for development of a second or third generation device.

Compliance with ethical standards

Conflict of interest The authors declare that they have no competing interest.

References

1. Martin SP, Lamb DJ, Lynch JM, Reddy SM (2003) Enzyme based determination of cholesterol using the quartz cristal acoustic wave sensor. Anal Chim Acta 487:91–100. https://doi.org/10.1016/S0003-2670(03)00504-X
2. Vidal JC, Espuelas J, Ruiz EG, Castillo JR (2004) Amperometric cholesterol biosensors based on the electropolymerisation of pyrrole and the electrocatalytic effect of Prussian-blue layers helped with self-assembled monolayers. Talanta 64:655–664. https://doi.org/10.1016/j.talanta.2004.03.038
3. Motonaka J, Faulkner LR (1993) Determination of cholesterol and cholesterol ester with novel enzyme microsensors. Anal Chem 65:3258–3261. https://doi.org/10.1021/ac00070a015
4. Zhou N, Wang J, Chen T, Yu Z, Li G (2006) Enlargement of gold nanoparticles on the surface of a self-assembled monolayer modified electrode**:** a mode in biosensor design. Anal Chem 78:5227–5230. https://doi.org/10.1021/ac0605492
5. Kumar A, Rajesh A, Chaubey SK, Malhotra BD (2001) Immobilization of cholesterol oxidase and potassium ferricyanide on dodecylbenzene sulfonate ion-doped polypyrrole film. J Appl Polym Sci 82:3486–3491. https://doi.org/10.1002/app.2210
6. Aravamudhan S, Kumar A, Mohapatra S, Bhansali S (2007) Sensitive estimation of total cholesterol in blood using Au nanowires based micro-fluidic platform. Biosens Bioelectron 22:2289–2294. https://doi.org/10.1016/j.bios.2006.11.027
7. Hasanzadeh M, Shadjou N, And de la Guardia M (2015) Iron and iron-oxide magnetic nanoparticles as signal-amplification elements in electrochemical biosensing. Trends Anal Chem 72:1–9. https://doi.org/10.1016/j.trac.2015.03.016
8. Pinho MS, Gregori ML, Nunes RCR, Soares BG (2001) Aging effect on the reflectivity measurements of polychloroprene matrices containing carbon black and carbonyl-iron powder. Polym Degrad Stab 73:1–5. https://doi.org/10.1016/S0141-3910(00)00198-1
9. Sieben S, Bergemann C, Lubbe A, Brockmann B, Rescheleit D (2001) Comparison of different particles and methods for magnetic isolation of circulating tumor cells. J Magn Mater 225:175. https://doi.org/10.1016/S0304-8853(00)01248-8
10. Abdelhamid HN (2019) Nanoparticle based surface assisted laser desorption ionisation mass spectrometry: a review. Microchim Acta 186:682. https://doi.org/10.1007/s00604-019-3770-5
11. Kouassi GK, Irudayaraj J, McCarty G (2005) Examination of cholesterol oxidase attachment to magnetic nanoparticles. J Nanobiotechnol 3:1. https://doi.org/10.1186/1477-3155-3-1
12. Lu BW, Chen WC (2006) A disposable glucose biosensor based on drop- coating of screen-printed carbon electrodes with magnetic nanoparticles. J Magn Magn Mater 304:e400–e402. https://doi.org/10.1016/j.jmmm.2006.01.222
13. Wang SF, Xie F, Hu RF (2007) Carbon-coated nickel magnetic nanoparticles modified electrodes as a sensor for determinationof acetaminophen. Sens Act B 123:495–500. https://doi.org/10.1016/j.snb.2006.09.031
14. Dong A, Ren N, Tang Y, Wang Y, Zhang Y, Hua W, Gao Z (2003) General synthesis of mesoporous spheres of metal oxides and buffers. J Am Chem Soc 125:4976–4977. https://doi.org/10.1021/ja029964b
15. Ahmad M, Pan C, Gan L, Nawaz Z, Zhu J (2010) Highly sensitive amperometric cholesterol biosensor based on Pt-incorporated fullerene-like ZnO nanospheres. J Phys Chem C 114:243–250. https://doi.org/10.1021/jp9089497
16. Huang Y, Cui L, Xue Y, Zhang S, Zhu N, Liang J, Li G (2017) Ultrasensitive cholesterol biosensor based on enzymatic silver deposition on gold nanoparticles modified screen-printed carbon electrode. Mater Sci Eng C 77:1–8. https://doi.org/10.1016/j.msec.2017.03.253
17. Dey RS, Raj CR (2010) Development of an amperometric cholesterol biosensor based on graphene−Pt nanoparticle hybrid material. J Phys Chem C 114:21427–21433. https://doi.org/10.1021/jp105895a
18. Sharma R, Sinha RK, Varun AV (2014) Electroactive Prussian blue encapsulated iron oxide nanostructures for mediator-free cholesterol estimation. Electroanalysis 26:1551–1559. https://doi.org/10.1002/elan.201400050
19. Ruecha N, Rangkupan R, Rodthongkum N (2014) Novel paper-based cholesterol biosensor using graphen /polyvinylpyrrolidone/polyaniline nanocomposite. Biosensor Bioelectron 52:13–19. https://doi.org/10.1016/j.bios.2013.08.018
20. Satvekar RK, Pawar SH (2018) Multienzymatic cholesterol nanobiosensor using core-shell nanoparticles incorporated silica nanoparticles. J Med Biol Eng 38:735–743. https://doi.org/10.1007/s40846-017-0345-y
21. Cornell RM, Schwertmann U, (2006) The iron oxides structures, properties, reactions, occurrences and uses. p 139-146. ISBN: 978-3-527-60644-3
22. Shaw SY, Chen YJ, Ou JJ, Ho L (2006) Preparation and characterization of Pseudomonas putida esterase immobilized on magnetic nanoparticles. EnzyMicrob Tech 39:1089–1095. https://doi.org/10.1016/j.enzmictec.2006.02.025
23. Pan BF, Gao G, Gu HC (2005) Dendrimer modified magnetite nanoparticles for protein immobilization. J Colloid Interface Sci 284:1–6. https://doi.org/10.1016/j.jcis.2004.09.073
24. Garcia-Ruiz EG, Vidal JC, Aramendia MT, Castillo JR (2004) Design of an interference-free cholesterol amperometric biosensor based on the electrosynthesis of polymeric films of diaminonaphthalene isomers. Electroanal. 16:497–504. https://doi.org/10.1002/elan.200302853
25. Salinas E, Rivero V, Torriero AAJ, Benuzzi D, Sanz MI, Raba J (2006) Multienzymatic-rotating biosensor for total cholesterol determination in a FIA system. Talanta 70:244–250. https://doi.org/10.1016/j.talanta.2006.02.043
26. Singh S, Solanki PR, Pandey MK, Malhotra BD (2006) Covalent immobilisation of cholesterol esterase and cholesterol oxidase on polyaniline films for application to cholesterol biosensor. Anal Chim Acta 568:126–132. https://doi.org/10.1016/j.aca.2005.10.008
27. Ahmadalinezhad A, Chen A (2011) High performance electrochemical biosensor for the detection of total cholesterol. Biosens Bioelectron 26:4508–4513. https://doi.org/10.1016/j.bios.2011.05.011
28. Shih W-C, Yang M-C, Lin MS (2009) Development of disposable lipid biosensor for the determination of total cholesterol. Biosens Bioelectron. 24:1679–1684. https://doi.org/10.1016/j.bios.2008.08.055
29. Malik V, Pundir CS (2002) Determination of total cholesterol in serum by cholesterol esterase and cholesterol oxidase immobilized and co-immobilized on to arylamine glass. Biotechnol Appl Biochem 35:191–197. https://doi.org/10.1111/j.1470-8744.2002.tb01188.x
30. Marazuela MD, Cuesta B, Bondi MCM, Quejido A (1997) Free cholesterol fiber-optic biosensor for serum samples with simplex optimization. Bios. Bioelectr 12:233–240. https://doi.org/10.1016/S0956-5663(97)85341-9